J Comput Aided Mol Des (2009) 23:209–225
DOI 10.1007/s10822-008-9252-1

Molecular modelling evaluation of the cytotoxic activity of podophyllotoxin analogues

Md. Afroz Alam · Pradeep Kumar Naik

Received: 20 August 2008 / Accepted: 15 November 2008 / Published online: 4 December 2008

Abstract Podophyllotoxin and its structural derivatives, a class of tubulin polymerization inhibitors, have been the objective of numerous studies to prepare better and safer anti-cancer drugs. A library of podophyllotoxin analogues has been designed consisting of 154 analogues. Their molecular interactions and binding affinities with tubulin protein (1SA1) have been studied using the docking-molecular mechanics based on generalized Born/surface area (MM-GBSA) solvation model. Quantitative structure activity relationships were developed between the cytotoxic activity (pIC_{50}) of these compounds and molecular descriptors like docking score and binding free energy. For both the cases the r^2 was in the range of 0.642–0.728 indicating good data fit and r^2_{cv} was in the range of 0.631–0.719 indicating that the predictive capabilities of the models were acceptable. In addition, a linear correlation was observed between the predicted and experimented pIC_{50} for the validation data set with correlation coefficient r^2 of 0.806 and 0.887, suggesting that the docked structure orientation and the interaction energies are reasonable. Low levels of root mean square error for the majority of inhibitors establish the docking and Prime/MM-GBSA based prediction model as an efficient tool for generating more potent and specific inhibitors of tubulin protein by testing rationally designed lead compounds based on podophyllotoxin derivatization.

Keywords Podophyllotoxin · Virtual screening · Molecular docking · Prime/MM-GBSA

Md. Afroz Alam · P. K. Naik (✉)
Department of Bioinformatics and Biotechnology, Jaypee University of Information Technology, Waknaghat, Solan 173215, Himachal Pradesh, India
e-mail: pknaik73@rediffmail.com

Introduction

Normal cell division, intracellular transport, cellular motility, cell signaling and maintenance of cell shape are all dependent on highly regulated dynamic instability process of the tubulin/microtubule system. Microtubules are hollow tubes consisting of α- and β-tubulin heterodimers that polymerize parallel to a cylindrical axis. Mitotic microtubules are very dynamic structures, switching between growing and shortening states, a process known as dynamic instability. Drugs that inhibit tubulin polymerization/depolymerization are commonly used as chemotherapeutic agents for a variety of cancer, as well as for probing microtubule dynamics in cellular and biochemical processes. Well-known examples are vinblastine, vincristine and paclitaxel. However, the mechanism of action of these microtubule poisons with tubulin is different. For example, paclitaxel, vinca alkaloids, colchicinoids and dolastatin appear to bind different sites on the tubulin α–β heterodimer [1].

Podophyllotoxin is clinically effective anti-cancer agent that represents perhaps the most significant addition to the pharmacopoeia of cancer chemotherapeutic agents in the last decade [2]. Prompted by the clinical successes of the podophyllotoxin, significant efforts have been focused on identifying new analogues that have a similar mechanism of action yet superior properties such as low or nil toxic side effects and better oral availability [3–5]. A consistent number of structural modifications have been introduced in the original structure of podophyllotoxin in order to overcome the side effects associated with its utilization as anti-cancer drug. The study and assessment of these have permitted the clinical development and their usage in the treatment of different types of cancer.

Since the discovery of the therapeutic properties of podophyllotoxin, new findings related to its activities, its

mechanism of action and pharmacological properties have been unveiled. Structure-Activity Relationships (SAR), have shown that podophyllotoxin analogues preferentially inhibit tubulin polymerization, which leads to arrest of the cell cycle in the metaphase [6, 7]. The first substance known to have this activity was colchicine, which binds to a specific site on the protein, known as the colchicine site. Different derivatives of podophyllotoxin have demonstrated to bind to the same site, as shown by the fact that podophyllotoxin has been reported to compete with colchicine for the binding site in tubulin [8], its affinity is more than double to that of colchicine. Furthermore, colchicine binds to tubulin almost irreversibly whereas podophyllotoxin derivatives do so reversibly, which makes them less toxic and more useful in the field of cancer therapy [9, 10]. The discovery of new natural and semi-synthetic compounds of podophyllotoxin being cytotoxic by interference with tubulin have attracted much attention in the last several years. The microtubule complex has thus proven to be a compelling target for the development of anti-cancer therapeutic agents [11, 12]. Crystal structures of tubulin with colchine and podophyllotoxin have been reported. The crystal structures show that all colchicines and podophyllotoxin bind at the interface between α and β subunit of tubulin protein. The binding site of tubulin-podophyllotoxin complex (PDB ID: 1SA1, $R = 4.20$ Å) consists of amino acids such as; Serα178, Thr α179, Ala α180, Val α181, Val β238, Cys β241, Leu β242, Ala β250, Lys β254, Leu β255, Asn β258, Met β259, Val β315, Ala β316, Ala β317, Val β318, Asn β350, Lys β352, and Ileu β378. Similar amino acid residues were also found in the binding site of tubulin-colchicine complex (PDB ID: 1SA0, $R = 3.58$ Å). Although the overall shape of the podophyllotoxin binding site is relatively the same in comparison to colchicine binding site, there are subtle differences among them (root mean square deviation (RMSD) = 1.29 Å). The hydrophobic center that is located in the middle of trimethoxyphenyl moiety of podophyllotoxin is surrounded by Leu β242, Ala β250, Leu β255, Ala β316, Val β318 and Ile β378 residues.

The great diversity of the podophyllotoxin analogues, the huge number of assays carried out on them, and the different mechanisms of action observed in different series make it difficult to clearly define the minimum structural requirements necessary for their biological activity. Additionally, the results available have been obtained by different authors; at different times using different technologies on very diverse types of tumours or cultures of neo-plastic cells. For all these reasons, greater systematization would be required to obtain definitive conclusions. The mechanism of action of any drug is very important in drug development. Generally, the drug compound binds with a specific target, a receptor, to mediate its effects. Therefore, suitable drug–receptor interactions are required for high activity. Understanding the nature of these interactions is very significant and theoretical calculations, in particular the molecular docking method, seem to be a proper tool for gaining such understanding. The docking results obtained will give information on how the chemical structure of the drug should be modified to achieve suitable interactions and for the rapid prediction and virtual prescreening of anti-tumour activity.

Given the mechanism of action of podophyllotoxin analogues two accepted mechanisms have been proposed. One consists of the inhibition of tubulin polymerization and the second accepted mechanism consisting of the irreversible inhibition of DNA-topoisomerase II [1, 9, 13]. Structure-Activity Relationships (SAR) studies reported earlier have shown that podophyllotoxin like compounds preferentially inhibit tubulin polymerization, which leads to arrest of the cell cycle in the metaphase [6, 7]. However, etoposide like compounds are potent irreversible inhibitors of DNA topoisomerase II and their action is based on the formation of a nucleic acid-drug-enzyme complex, which includes single and double stranded DNA breaks that eventually lead to cell death [7, 14].

In this work we created a virtual library of podophyllotoxin analogues which were collected from different sources and screened them for tubulin binding. Further, prediction models for predicting the cytotoxic activity of these compounds were developed based on binding interaction with tubulin as descriptor. This prediction model was used for predicting the cytotoxic activity of newly developed analogues. We have used the molecular modelling techniques (molecular docking and rescoring using Prime/MM-GBSA) to find the series of podophyllotoxin analogues that should be modified for energetically favourable interaction with tubulin and for better cytotoxic activity.

Materials and methods

Preparation of protein

The X-ray structure of the complex between podophyllotoxin and tubulin protein (PDB ID: 1SA1) has been used as initial structure in the preparation of podophyllotoxin binding site. After manual inspection and cleaning of structure we retained a complex consisting of protein chains α and β and podophyllotoxin ligand. Hydrogens were added to the model automatically via the Maestro interface [15] leaving no lone pair and using an explicit all-atom model. All the water molecules were removed form the complex. The multi step Schrodinger's protein preparation tool (PPrep) has been used for final preparation of

protein. PPrep neutralized side chains that are not close to the binding cavity and do not participate in salt bridges [15]. This step is then followed by restrained minimization of co-crystallized complex, which reorients side chain hydroxyl groups and alleviates potential steric clashes. Progressively weaker restraints (tethering force constants 3, 1, 0.3, 0.1) were applied to non-hydrogen atoms only. The complex obtained was minimized using OPLS-2005 force field with Polack-Ribiere Conjugate Gradient (PRCG) algorithm [16]. The minimization was stopped either after 5,000 steps or after the energy gradient converged below 0.05 kcal/mol.

Virtual library design

The virtual library of podophyllotoxin analogues contains 154 compounds divided into five sub libraries. All these compounds are taken from various sources belonging to different ring modifications.

Sublib-I commonly known as tetralinelactones consists of 52 compounds (1–52) (Table 1). These molecules were rationally designed as functional mimics of natural podophyllotoxin with the goal of simplifying the chemical synthesis and improving the cytotoxic activity. Structural modification mainly introduced varying radicals at position 7 in podophyllotoxin scaffold. Reports have been made of compounds with oxygenated substituents in the form of ethers, esters and diverse nitrogen radicals [17–26].

Sublib-II contains compounds (53–97) (Table 2) commonly known as non-lactonic tetralines. Structural modifications in this group include the opening of the lactone ring (D-ring) in podophyllotoxin scaffold, to give rise to compounds with different degrees of oxidation at positions C-9 and C-9′ [19–22, 24, 25]. In general these molecules lack lactones ring.

Sublib-III also includes a group of lignans (98–120) (Table 3) that have heterocyclic rings fused to the cyclolignan skeleton. This group is commonly called as pyrazolignans [19, 20, 24, 25, 27] and isoxazolignans [25, 26, 28, 29] and they were obtained by reacting podophyllotoxine with differently substituted hydrazines and hydroxylamines.

Sublib-IV includes the compounds (121–126) (Table 4) commonly called lactonic and non-lactonic naphthalene. These molecules were obtained by structural modification of C and D-rings and have proportionally much lower activity [19, 20, 24].

Sublib-V contains compounds (127–154) (Table 5) commonly known as aza-podophyllotoxin analogues. The preparation of this group of compounds requires selective chemical manipulation of the two aromatic rings (B and E-rings) of the podophyllotoxin scaffold. These molecules are readily prepared from anilines, benzaldehydes and tetronic acid or 2,3-cyclopentanedione in good to excellent yield and have also shown better cytotoxic activity [30].

The virtual library of podophyllotoxins was built from the scaffolds by different ring modification and substitution of functional groups as mentioned in Tables 1, 2, 3, 4, 5. We used ISIS Draw 2.3 software for sketching structures and converting them to their 3D representation by using ChemSketch 3D viewer of ACDLABS 8.0. LigPrep [15] was used for final preparation of ligands from libraries for docking. LigPrep is a utility of Schrodinger software suit that combines tools for generating 3D structures from 1D (Smiles) and 2D (SDF) representation, searching for tatutomers and steric isomers and perform a geometry minimization of ligands. The ligands were minimized by means of Molecular Mechanics Force Fields (OPLS-2005) with default setting.

Docking procedure

The Schrodinger Glide program version 4.0 has been used for docking [31, 32]. The best 10 poses and corresponding scores have been evaluated using Glide in single precision mode (Glide SP) for each ligand from the virtual library of podophyllotoxin. For each screened ligand, the pose with the lowest Glide SP score has been taken as the input for the Glide calculation in extra precision mode (Glide XP). To soften the potential for non-polar parts of the receptor, we scaled van der Waals radii of receptor atoms by 1.00 with partial atomic charge 0.25.

Rescoring using Prime/MM-GBSA approach

For each ligand, the pose with the lowest Glide score was rescored using Prime/MM-GBSA approach [33]. This approach is used to predict the free energy of binding for set of ligands to receptor. The docked poses were minimized using the local optimization feature in Prime and the energies of complex were calculated using the OPLS-AA force field and generalized-Born/surface area (GB/SA) continuum solvent model. The binding free energy (ΔG_{bind}) is then estimated using equation:

$$\Delta G_{\text{bind}} = E_{\text{R:L}} - (E_{\text{R}} + E_{\text{L}}) + \Delta G_{\text{solv}} + \Delta G_{\text{SA}} \quad (1)$$

where $E_{\text{R:L}}$ is energy of the complex, $E_{\text{R}} + E_{\text{L}}$ is sum of the energies of the ligand and unliganded receptor, using the OPLS-AA force field, ΔG_{solv} (ΔG_{SA}) is the difference between GBSA solvation energy (surface area energy) of complex and sum of the corresponding energies for the ligand and unliganded protein. Corrections for entropic changes were not applied in this type of free energy calculation.

In order to explore the reliability of the proposed models we used the cross validation method. The cross validation analysis performed by using the leave one out (LOO)

Table 1 Podophyllotoxin derivatives (Tetralactones) with cytotoxic activities against P-388 cell line as well as new proposed structural derivatives with unknown cytotoxic activity used in the work

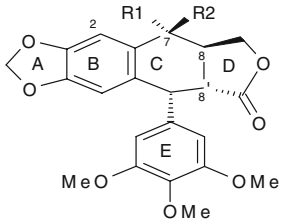

1-22

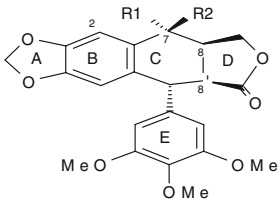

23-42

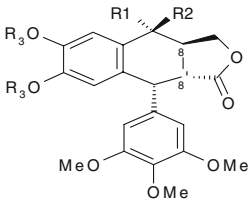

45-52

Analogue	R1	R2	IC_{50}(μM)	Analogue	R1	R2	IC_{50}(μM)
1	OH	H	0.012	22		=N-OMe	0.2
2	H	H	0.010	23	H	H	0.10
3	H	H(2-OMe)	0.01	24	H	H(2-OMe)	0.23
4	OH	H(2-OMe)	-	25	OH	H	6.0
5	OH	H(4'-OH	0.027	26	OH	H(2-OMe)	-
6	OAc	H	0.625	27	OAc	H	0.55
7	OAc	H	-	28	OAc	H(2-OMe)	1.02
8	OMe	H	0.06	29	OMe	H	0.12
9	H	OH	0.06	30	H	OH	-
10	H	Ac	0.05	31	H	OH(2-OMe)	0.11
11	H	OMe	0.06	32	H	OAc	0.44
12	H	Cl	0.6	33	H	OAc(2-OMe)	0.51
13	Cl	H	0.6	34	H	OMe	0.12
14		=O	1.8	35	H	Cl	-
15	H	Br	-	36	Cl	H	-
16	Br	H	-	37	H	H ? $^{8(8')}$	-
17	H	H(4'-OH)	-	38	H	H ? ^{7}	0.013
18	H	H(4'-OAc)	-	39	=O	12.0	
19	H	OAc(4'-OAc)	-	40		=N-OH	2.3
20		= N-OH	2.3	41		N-OAc	-
21		=N-OAc	2.1	42		=N-OMe	2.3
43	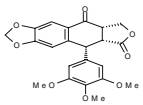		-	44	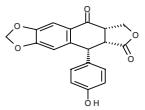		-

Analogue	R1	R2	R3	IC_{50}(μM)	Analogue	R1	R2	R3	IC_{50}(μM)
45	H	H	H	-	49	H	OH	H	-
46	H	H	Ac	-	50	H	OAc	Ac	-
47	OH	H	H	-	51	H	H	H $\Delta^{8(8')}$	-
48	OAc	H	Ac	-	52	H	H	Ac $\Delta^{8(8')}$	-

method in which one compound removed from the data set and its activity predicted using the model derived from the rest of the data points. Prediction error sum of squares (PRESS) is a standard index to measure the accuracy of a modelling method based on the cross validation technique. The r^2_{cv} was calculated based on the *PRESS* and *SSY* (Sum of squares of deviations of the experimental values from their mean) using following formula.

$$r^2_{cv} = 1 - \frac{\text{PRESS}}{\text{SSY}} = 1 - \frac{\sum_{i=1}^{n} (y_{exp} - y_{pred})^2}{\sum_{i=1}^{n} (y_{exp} - \bar{y})^2} \quad (2)$$

where y_{exp}, y_{pred} and $\bar{y}$ are the observed, predicted and mean values of the cytotoxic activities of the podophyllotoxin analogues.

Table 2 Podophyllotoxin derivatives (Nonlactonic tetralines) with cytotoxic activities against P-388 cell line as well as new proposed structural derivatives with unknown cytotoxic activity used in the work

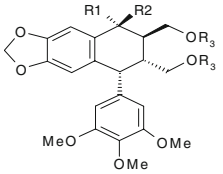

53 - 59.

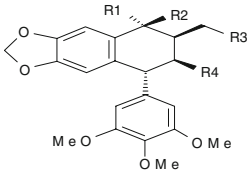

62-81

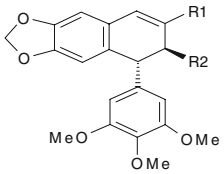

82 - 92.

Analogue	R1	R2	R3	IC_{50}(μM)	Analogue	Structure	IC_{50}(μM)
53	OH	H	H	1.2	60	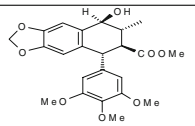	23.3
54	H	OH	H	12.0			
55	H	OAc	Ac	-			
56	H	OMe	H	11.6			
57	H	OMe	Ac	9.7			
58	OMe	H	H	-	61	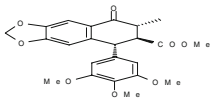	3.5
59	OMe	H	Ac	9.7			

Analogue	R1	R2	R3	R4	IC_{50}(μM)	Analogue	R1	R2	R3	R4	IC_{50}(μM)
62	H	H	OH	COOMe	0.058	71	H	OMe	OH	CH_2OH	11.6
63	H	H	OAc	COOMe	0.21	72	H	OMe	OAc	CH_2OAc	9.7
64	H	H	OAc	CH_2OAc	5.14	73	H	OH	OH	CH_2OH	47.9
65	OH	H	OH	CH_2OH	23.9	74	H	OH	OH	COOMe	1.1
66	OH	H	OH	COOMe	0.22	75	=O		OH	COOMe	5.63
67	OAc	H	OAc	CH_2OAc	7.4	76	=O		OAc	COOMe	0.20
68	OAc	H	OAc	COOMe	1.1	77	=N-OH		OAc	COOMe	2.0
69	OMe	H	OH	CH_2OH	23.2	78	H	H	CHO	COOMe	2.34
70	OMe	H	OAc	CH_2OAc	19.4	79	H	H	=N-OMe	COOMe	2.30
80	H	H	=N-OMe	COOMe	10.94	81	H	H	=N-allyl	COOMe	2.5

Analogue	R1	R2	IC_{50}(μM)	Analogue	R1	R2	IC_{50}(μM)
82	CH_2OH	COOMe	0.02	89	CH=N-OH	COOMe	2.27
83	CHO	CH_2OH	0.25	90	CH=N-OMe	COOMe	0.22
84	CHO	COOMe	0.23	91		COOMe	0.20
85	CH=N-NH2	COOMe	0.57	92		CH_2OH	1.00
86	CH=N-NH-CH_2CF_3	COOMe	0.48	93	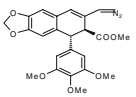		0.57
87	CH=N-NH-Ph	COOMe	1.94	94	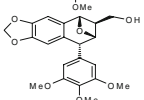		6.25
88	CH=N-NH-Ph	CH_2OH	1.02	95	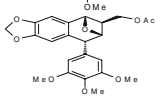		5.66
96	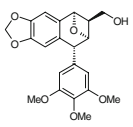		-	97	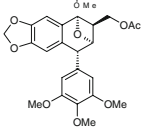		-

Table 3 Podophyllotoxin derivatives (Pyrazolignans and isoxazolignan) with cytotoxic activities against P-388 cell line as well as new proposed structural derivatives with unknown cytotoxic activity used in the work

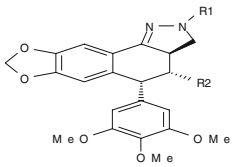

98 - 109.

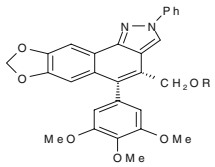

110-111

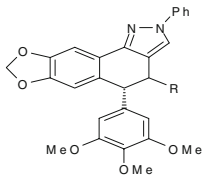

112-114

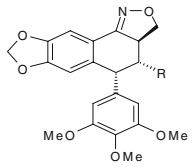

115-120

Analogue	R1	R2	IC_{50} (μM)	Analogue	R1	R2	IC_{50} (μM)
98	Ph	COOH	1.9	104	p-BrPh	COOH	–
99	Ph	COOMe	1.00	105	p-MePh	COOMe	1.00
100	Ph	CH_2OH	4.1	106	Me	COOH	–
101	Ph	CH_2OAc	4.7	107	Me	COOMe	5.6
102	m-NO_2Ph	COOH	–	108	CONH2COOH	COOH	–
103	m-NO_2Ph	COOMe	4.5	109	$COCH_3COOMe$	COOMe	21

Analogue	R	IC_{50} (μM)	Analogue	R	IC_{50} (μM)
110	H	10	116	COOMe	23
111	Ac	–	117	COOMe(4′-OH)	12
112	CHO	21	118	CH_2OH	2.6
113	CH_2OH	–	119	CH_2O	2.4
114	CH_2Ac	2.2	120	CHO	–
115	COOH	2.2			

Table 4 Podophyllotoxin derivatives (lactones and non-lactonic naphthalene) with cytotoxic activities against P-388 cell line used in the work

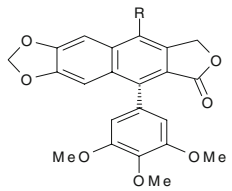

121-122

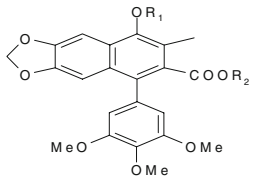

123-126

Analogue	R	IC_{50} (μM)	Analogue	R1	R2	IC_{50} (μM)
			123	H	Me	12.20
121	H	5.1	124	Ac	H	5.90
122	OAc	44.25	125	Ac	Me	16.59
			126	H	OMe	2.15

Results and discussions

Molecular docking of podophyllotoxin and its analogues

The original crystal structure of tubuline-podophyllotoxin complex (PDB ID: 1SA1) was used to validate the Glide-XP docking protocol. This was done by moving the co-crystallized podophyllotoxin ligand outside of active site and then docking it back into the active site. The top 10 configurations after docking were taken into consideration to validate the result (Table 6). The RMSD was calculated for each configuration in comparison to the co-crystallized podophyllotoxin and the value was found to be in between 0.02–0.85 Å. Whereas the RMSD value calculated out of ten accepted poses for each configuration was found in between 0.59–1.33 Å. This revealed that the docked configurations have similar binding positions and orientations within the binding site and are similar to the crystal structure. The best docked structures, which is the configuration with the lowest Glide score is compared with the crystal structure as shown in Fig. 1. These docking results illustrate that the best-docked podophyllotoxin complex agrees well with its crystal structure and that Glide (XP)-docking protocol successfully reproduces the crystal tubulin-podophyllotoxin complex.

Glide 4.0 in XP mode have been used to dock the library (I–V) into the podophyllotoxin binding site of tubulin. The docking score (G-score) has been used for screening the virtual library of podophyllotoxin analogues. The binding modes of five superimposed ligands from each class within podophyllotoxin binding site are given in Fig. 2a–e

Table 5 Aza-podophyllotoxin derivatives with cytotoxic activities against P-388 cell line used in the work

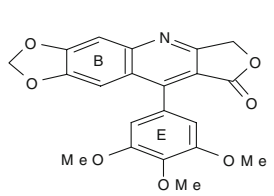

Modification 1

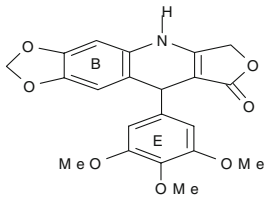

Modification 2

Substitution of B & E ring at 1 and 2 analogues:

Modification 1				Modification 2			
Analogue	B Ring	E Ring	IC_{50}(μM)	Analog	B Ring	E Ring	IC_{50}(μM)
127	I	VII	100	141	I	VII	0.0018
128	II	VII	80	142	II	VII	0.0017
129	III	VII	100	143	III	VII	4.9
130	III	VIII	39	144	III	VIII	0.76
131	III	XII	2.0	145	III	XII	0.77
132	IV	VII	29	146	IV	VII	2.6
133	V	VII	100	147	V	VII	0.0041
134	VI	VII	63	148	VI	VII	0.92
135	I	VIII	40	149	I	VIII	0.048
136	I	IX	100	150	I	IX	0.0053
137	I	X	100	151	I	X	0.13
138	I	XI	60	152	I	XI	0.0053
139	I	XII	100	153	I	XII	0.030
140	I	VII	71	154	I	VII	0.028

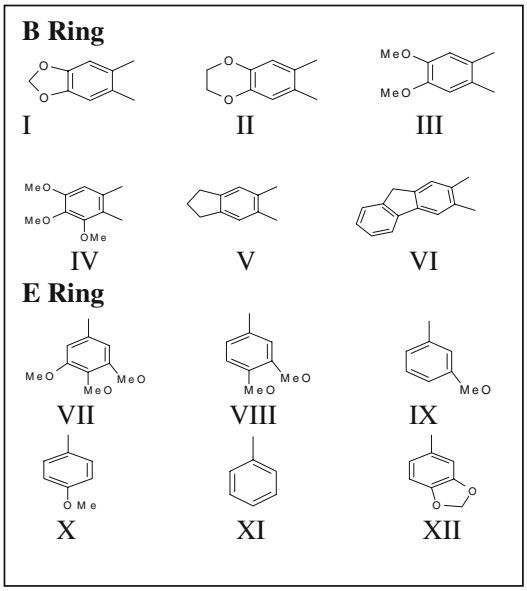

Table 6 The RMSD and docking score from the docking simulation of 10 lowest configurations of co-crystal podophyllotoxin in Tubuline protein (ISA1)

Configuration	Glide score	ΔG^{a}_{score}	RMSD[b] (Å)	RMSD[c] (Å)
1	−10.26	0	0.85	0.60
2	−10.20	−0.06	0.02	0.86
3	−9.80	−0.46	0.68	1.33
4	−9.72	−0.54	0.57	1.26
5	−9.50	−0.76	0.04	0.67
6	−9.25	−1.01	0.04	0.67
7	−8.78	−1.48	0.80	0.59
8	−8.47	−1.79	0.13	1.02
9	−7.87	−2.39	0.03	0.79
10	−7.72	−2.54	0.07	0.90

[a] $\Delta G_{score} = E_i - E_{lowest}$, [b] *RMSD* RMSD between docked and crystallographic podophyllotoxin structure, [c] *RMSD* RMSD between docked poses corresponding to each configuration

respectively. In this figure we can observe that all the ligands are well fitted to the defined binding pocket. All the 154 podophyllotoxin analogues were found to be good binder with tubulin. For each ligand in the virtual library, the pose with the lowest Glide score was rescored using Prime/MM-GBSA approach. This approach is used to predict the binding free energy (ΔG_{bind}) for set of ligands to receptor.

Building models for prediction of pIC_{50} using Glide score and Prime/MM-GBSA energy

We selected some ligands with known cytotoxic activity (pIC_{50}) from virtual library (I–V). Cytotoxic activity of these podophyllotoxin analogues (Sublib I–V) was generally evaluated using P-388 leukemia cells and were collected from different sources [30, 34, 35] and included in Tables 1, 2, 3, 4, and 5. It has been seen that the dihydroquinoline analogues (127–154) belonging to aza-podophyllotoxin (sublib-V) have significantly better activitives (pIC_{50} in the range of −2.00–2.77 μM) compared to the other sublibraries (I–IV). On the contrary, the tetralinelactones (1–52 analogues; sublib-I) showed comparatively better activity of pIC_{50} value ranging from −1.08 μM to 2.00 μM than

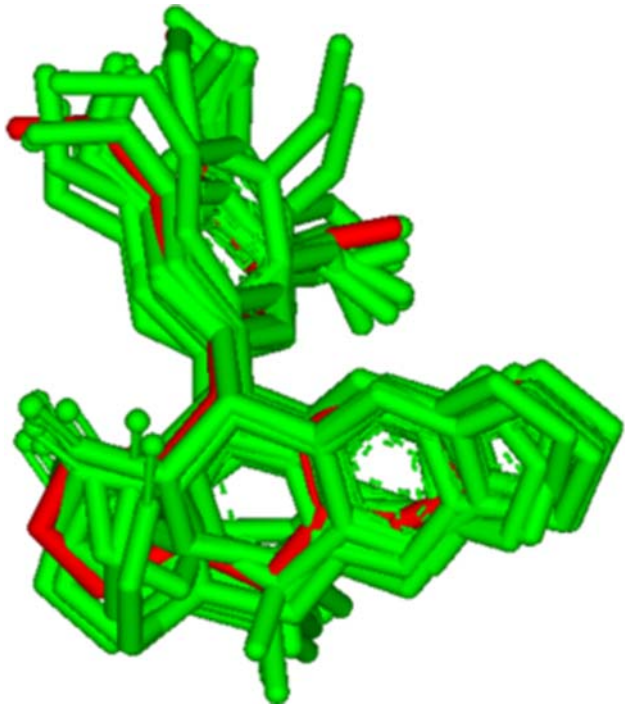

Fig. 1 Superposition of all docked configurations of podophyllotoxin on crystal structure (*red-stick*). RMSD (heavy atoms) = 0.02–0.85 Å

non-lactonic tetralines (sublib-II). The pyrazolignans and isoxazolignans, lactonic and non-lactonic naphthalene generally showed very weak or no activity. The mode of action of podophyllotoxin structural derivatives is reported to be due to inhibition of microtubule assembly through binding to tubulin [1, 2]. Thus, in this study we have taken tubulin protein as the molecular target and built prediction model for prediction of cytotoxic activity by considering the Glide score and ΔG_{bind} as descriptors. The Eq. (3) of the model and the corresponding statistics are shown below:

$$pIC_{50} = -8.725(\pm 0.644) - 0.938(\pm 0.592) \times \text{G-score} \quad (3)$$

$N = 120$, $r^2 = 0.642$, $s = 0.692$, $F = 211.86$, $r^2_{cv} = 0.631$, PRESS = 58.349.

The root mean square error (RMSE) between the experimental pIC_{50} values and the predicted pIC_{50} values obtained by the regression model was 0.626 μM, which is an indicator of the robustness of the fit and suggested that the calculated pIC_{50} based on Glide score is reliable. The quality of the fit can also be judged by the value of the squared correlation coefficient (r^2), which was 0.642 for the data set. Figure 3 graphically shows the quality of fit. The statistical significance of the prediction model is evaluated by the correlation coefficient r^2, standard error, *F*-test value, leave-one-out cross-validation coefficient r^2_{cv} and predictive error sum of squares PRESS. The regression model developed in this study is statistically ($r^2_{cv} = 0.631$, $r^2 = 0.642$, $F = 211.86$) best fitted and consequently used for prediction of cytotoxic activities (pIC_{50}) of the podophyllotoxin analogues as reported in Table 7. The average root mean square error between predicted and experimental pIC_{50} values was 0.838 μM using leave-one-out cross validation technique which further revealed the reliability of the model for prediction of cytotoxicity.

We have used Prime/MM-GBSA protocol for rescoring Glide XP poses of the podophyllotoxin analogues. From the results collected in Table 7 we didn't find correlation between Glide score and ΔG_{bind} energy ($r^2 = 0.3175$) (Fig. 4). However, we did find a better correlation between ΔG_{bind} energy and experimental pIC_{50} ($r^2 = 0.7285$) (Fig. 5). Rescoring using Prime/MM-GBSA leads to minor changes of the ligand conformations (due to energy minimization of the ligand in receptor's environment) and consequent stabilization of receptor and ligand complex. A linear regression model for prediction of predicted pIC_{50} of cytotoxicity has been developed by considering some analogues with known pIC_{50}. In this model we have taken ΔG_{bind} energy as a descriptor. The Eq. 4 of the model and the corresponding statistics are shown below:

$$pIC_{50} = -2.604(\pm 0.008) - 0.143(\pm 0.148) \times \Delta G_{bind} \quad (4)$$

$N = 120$, $r^2 = 0.728$, $s = 0.603$, $F = 316.58$, $r^2_{cv} = 0.719$, PRESS = 44.415.

The statistical significance of the prediction model is evaluated by the correlation coefficient r^2, standard error, *F*-test value, leave-one-out cross-validation coefficient r^2_{cv} and predictive error sum of squares PRESS. The regression model developed based on ΔG_{bind} energy is statistically ($r^2_{cv} = 0.719$, $r^2 = 0.728$, $F = 316.58$) best fitted and consequently used for prediction of cytotoxic activities (pIC_{50}) of the podophyllotoxin analogues as reported in Table 7. The average root mean square error between predicted and experimental pIC_{50} values was 0.770 μM by using leave-one-out cross validation technique which further revealed the reliability of the model for prediction of cytotoxicity. However, we may observe that model using ΔG_{bind} descriptors are better for predicting cytotoxicity (pIC_{50}) with a root mean square error of 0.575 μM than model using Glide score as a descriptor.

To judge the accuracy of the prediction models developed based on Glide score and ΔG_{bind} energy for predicting tubulin polymerization inhibition potencies, we have taken a separate data set called as validation test consisting of 16 compounds (Table 8). Their potencies and chemical structures were obtained from literature [36, 37]. Experimentally determined relative potencies of the drugs based on in vitro study are also provided in order to evaluate the accuracy of predictions. For all compounds, both the prediction models (Eqs. 3, 4) produce exactly the same trend for relative potencies, even though the exact magnitudes of

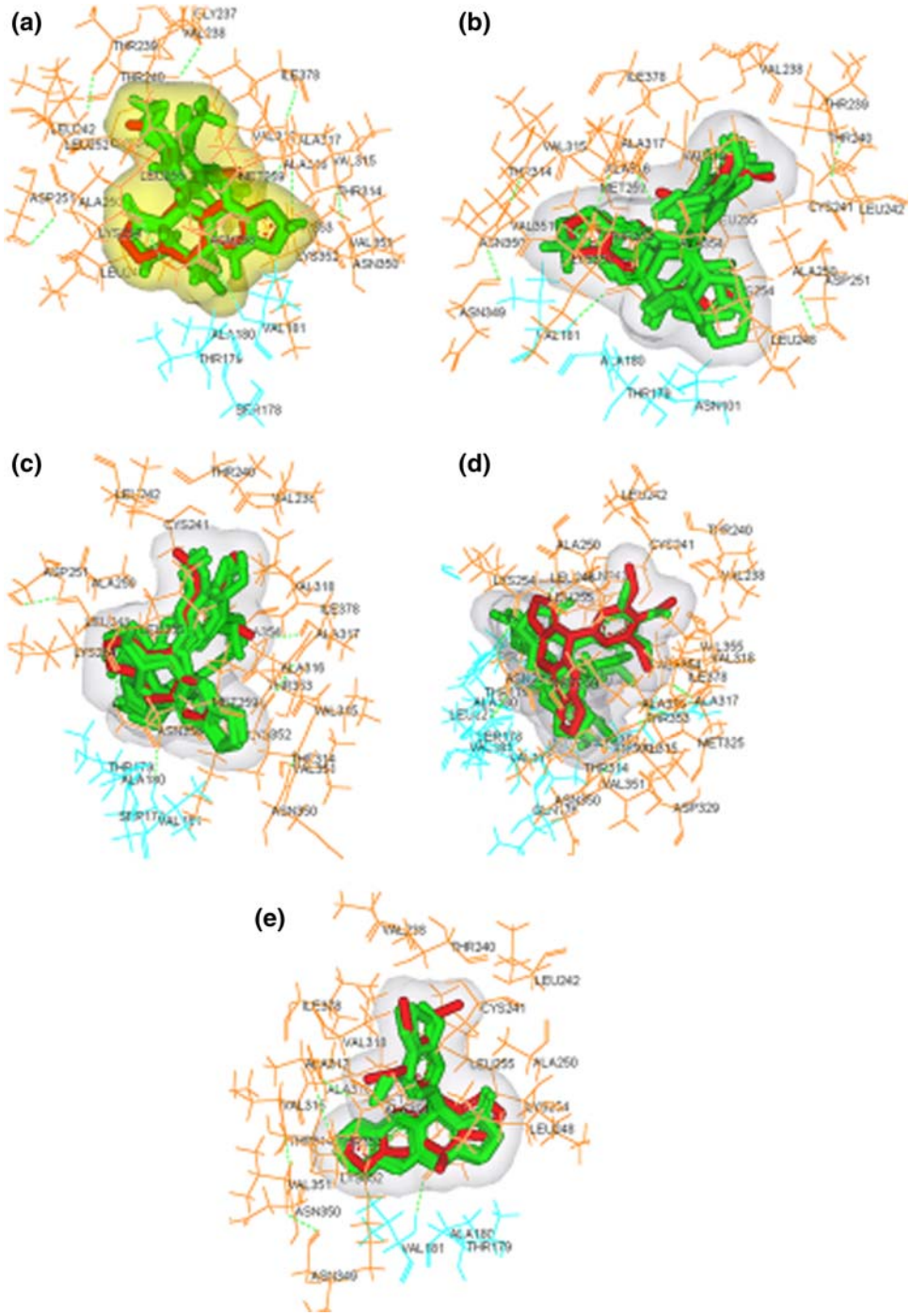

Fig. 2 Superposition of podophyllotoxin analogues (5 analogues) belonging to (**a**) Tetraline lactones, (**b**) Non-lactonic tetralines, (**c**) Pyrazoline and isoxazoline derivatives, (**d**) Lactonic and non-lactonic naphthaline and (**e**) Aza-podophyllotoxin derivatives within binding site of Tubuline along with the co-crystal podophyllotoxin (*red color*)

these values do not match very well (Table 9). The overall RMSE between the experimental and predicted pIC_{50} value was 0.27 and 0.25 μM, respectively by using Glide score and ΔG_{bind} energy, which means that the docking and Prime/MM-GBSA modeling was able to predict the cytotoxic activity of 16 podophyllotoxin analogues more reliably. Figure 6a, b graphically shows the quality of fit for the validation set.

Biological significance

The podophyllotoxin structural derivatives available till now belong either to only A, B, C, D, E or combination of ring modifications resulting in wide range of cytotoxicity activity. The modifications involving the C and D rings (lactone ring) gave the most promising results on activity [35]. Reports have been made of *cis* and *trans*-lactones

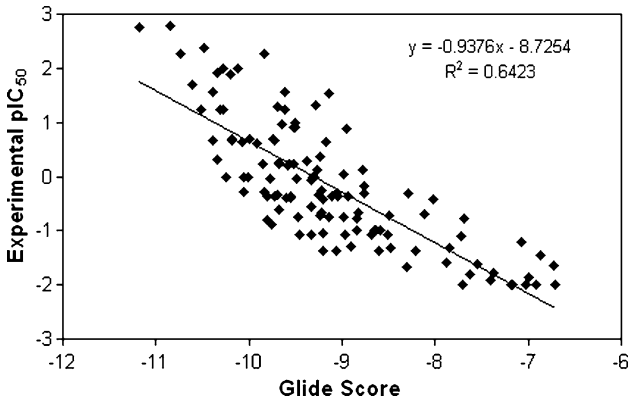

Fig. 3 Models for predicting cytotoxic activity (pIC_{50}) of the podophyllotoxin analogues based on Glide score

isomers, appearing either naturally or synthesized by transformations and inter-conversions [17, 18, 38]. Furthermore, within the lactonic group those compounds displaying a *trans*-junction between the tetraline and lactone fragments were more potent than their *cis*-analogues [19, 20, 24]. Based on docking study and rescoring using Prime/MM-GBSA we have seen that the *trans*-lactones have more negative Glide score and ΔG_{bind} energy value in comparison to *cis*-lactones. The observed differences in ΔG_{bind} energy and Glide score between *trans*- and *cis*-lactones could be explained in terms of their conformation and spatial arrangement of the lactone ring in relation to the other fused rings. Whereas, in the *trans*-lactones the four rings are almost co-planar, in the main conformer of *cis*-derivatives the lactone adopts an almost perpendicular disposition with respect to the other three rings. Both Glide score and ΔG_{bind} energy revealed that the lactonic group of podophyllotoxin ligands binds to tubulin protein with high affinity and showed better activity (Table 7). In general the non-lactonic group of podophyllotoxin analogues is less potent as anti-tumour agents. The Glide score and ΔG_{bind} energy of these

Table 7 Predicted cytotoxic activities of Tetralinelactones podophyllotoxin (a), nonlactonic tetralinelactones podophyllotoxin (b), pyrazolignans and Isoxazolignans podophyllotoxin (c), lactonic and non-lactonic naphthalene podophyllotoxin (d), Aza-podophyllotoxin (e) analogues using Glide score (XP) and Prime/MM-GBSA energy as a descriptor and experimental activity for selected analogues

Ligand	Glide score	ΔG_{bind} (kcal/mol)	Expt. pIC_{50}	Pred. pIC_{50}[a] (G-score)	Pred. pIC_{50}[b] (ΔG_{bind})	Ligand	Glide score	ΔG_{bind} (kcal/mol)	Expt. pIC_{50}	Pred. pIC_{50}[a] (G-score)	Pred. pIC_{50}[b] (ΔG_{bind})
(a)											
1	−10.34	−30.82	1.92	0.97	1.80	27	−9.67	−17.31	0.26	0.34	−0.13
2	−10.12	−32.00	2.00	0.76	1.97	28	−9.31	−15.33	−0.01	0.01	−0.41
3	−10.27	−31.27	2.00	0.91	1.87	29	−9.53	−18.28	0.92	0.21	0.01
4	−9.19	−2.41	–	−0.11	−2.26	30	−10.29	−26.96	–	0.92	1.25
5	−10.38	−26.93	1.57	1.01	1.25	31	−9.65	−21.00	0.96	0.32	0.40
6	−9.59	−19.70	0.20	0.27	0.21	32	−9.23	−14.44	0.36	−0.07	−0.54
7	−9.21	−21.20	–	−0.09	0.43	33	−9.37	−15.07	0.29	0.06	−0.45
8	−10.32	−27.45	1.22	0.95	1.32	34	−9.50	−19.51	0.92	0.19	0.19
9	−10.29	−26.97	1.22	0.92	1.25	35	−9.53	−26.13	–	0.21	1.13
10	−9.70	−27.86	1.30	0.37	1.38	36	−9.50	−27.53	–	0.19	1.33
11	−9.62	−27.35	1.22	0.29	1.31	37	−9.41	−23.36	–	0.10	0.74
12	−9.52	−18.36	0.22	0.20	0.02	38	−10.20	−29.07	1.89	0.84	1.55
13	−9.57	−17.24	0.22	0.24	−0.14	39	−8.68	−3.35	−1.08	−0.59	−2.12
14	−9.22	−10.42	−0.26	−0.08	−1.11	40	−9.05	−12.05	−0.36	−0.24	−0.88
15	−9.43	−4.85	–	0.12	−1.91	41	−10.48	−12.44	–	1.10	−0.82
16	−9.34	−7.34	–	0.03	−1.55	42	−9.11	−2.69	−0.36	−0.18	−2.22
17	−9.54	−21.20	–	0.22	0.43	43	−9.54	−12.68	–	0.22	−0.79
18	−9.73	−26.74	–	0.40	1.22	44	−9.56	−18.70	–	0.24	0.07
19	−10.01	−22.89	–	0.66	0.67	45	−9.56	−14.03	–	0.24	−0.60
20	−8.94	−3.87	−0.36	−0.34	−2.05	46	−9.89	−8.92	–	0.55	−1.33
21	−8.77	−9.15	−0.32	−0.51	−1.30	47	−8.97	−10.19	–	−0.31	−1.15
22	−9.74	−19.00	0.70	0.41	0.11	48	−10.53	−20.85	–	1.15	0.38
23	−9.51	−23.13	1.00	0.19	0.70	49	−9.33	−9.28	–	0.02	−1.28
24	−9.18	−19.22	0.64	−0.12	0.14	50	−9.29	−12.43	–	−0.02	−0.83
25	−8.84	−6.00	−0.78	−0.44	−1.75	51	−9.33	−16.24	–	0.02	−0.28
26	−9.08	−7.24	–	−0.22	−1.57	52	−10.81	−8.44	–	1.41	−1.40

Table 7 continued

Ligand	Glide score	ΔG_{bind} (kcal/mol)	Expt. pIC_{50}	Pred. pIC_{50}[a] (G-score)	Pred. pIC_{50}[b] (ΔG_{bind})	Ligand	Glide score	ΔG_{bind} (kcal/mol)	Expt. pIC_{50}	Pred. pIC_{50}[a] (G-score)	Pred. pIC_{50}[b] (ΔG_{bind})
(b)											
53	−9.33	−19.72	−0.08	0.02	0.22	76	−9.99	−7.44	0.70	0.64	−1.54
54	−9.34	−6.60	−1.08	0.03	−1.66	77	−9.06	−18.77	−0.30	−0.23	0.08
55	−10.15	−10.12	–	0.79	−1.16	78	−9.56	−18.58	−0.37	0.24	0.05
56	−8.97	−5.00	−1.06	−0.32	−1.89	79	−9.80	−16.42	−0.36	0.46	−0.26
57	−10.43	−3.07	−0.99	1.05	−2.16	80	−9.20	−20.09	−1.04	−0.10	0.27
58	−9.73	−1.65	–	0.40	−2.37	81	−9.60	−11.89	−0.40	0.27	−0.90
59	−8.85	−5.47	−0.99	−0.43	−1.82	82	−10.61	−11.74	1.70	1.22	−0.92
60	−9.20	−8.21	−1.37	−0.10	−1.43	83	−9.92	−29.53	0.60	0.57	1.62
61	−9.33	−3.74	−0.54	0.02	−2.07	84	−10.08	−19.15	0.64	0.73	0.13
62	−10.51	−15.51	1.24	1.13	−0.39	85	−9.86	−20.75	0.24	0.52	0.36
63	−10.19	−27.26	0.68	0.83	1.29	86	−10.34	−12.83	0.32	0.97	−0.77
64	−9.24	−20.00	−0.71	−0.06	0.26	87	−10.06	−25.00	−0.29	0.71	0.97
65	−8.60	−13.11	−1.38	−0.66	−0.73	88	−10.06	−12.69	−0.01	0.71	−0.79
66	−9.72	−8.56	0.66	0.39	−1.38	89	−9.72	−14.66	−0.36	0.39	−0.51
67	−9.77	−17.47	−0.87	0.43	−0.11	90	−10.39	−14.06	0.66	1.02	−0.59
68	−9.49	−15.16	−0.04	0.17	−0.44	91	−10.18	−23.40	0.70	0.82	0.74
69	−9.07	−10.38	−1.37	−0.22	−1.12	92	−9.30	−19.72	0.00	0.00	0.22
70	−8.91	−6.89	−1.29	−0.37	−1.62	93	−9.68	−17.67	0.24	0.35	−0.08
71	−9.46	−11.48	−1.06	0.15	−0.96	94	−9.80	−21.70	−0.80	0.46	0.50
72	−8.58	−12.83	−0.99	−0.68	−0.77	95	−9.48	−9.09	−0.75	0.16	−1.30
73	−8.30	−9.98	−1.68	−0.94	−1.18	96	−9.39	−14.60	–	0.08	−0.52
74	−9.78	−6.13	−0.04	0.44	−1.73	97	−9.48	−13.98	–	0.16	−0.60
75	−8.99	−15.85	−0.75	−0.30	−0.34						

Ligand	Glide score	ΔG_{bind} (kcal/mol)	Expt. pIC_{50}	Pred. pIC_{50}[a] (G-score)	Pred. pIC_{50}[b] (ΔG_{bind})	Ligand	Glide s core	ΔG_{bind} (kcal/mol)	Expt. pIC_{50}	Pred. pIC_{50}[a] (G-score)	Pred. pIC_{50}[b] (ΔG_{bind})
(c)											
98	−9.83	−19.79	−0.28	0.49	0.23	110	−8.65	−13.10	−1.00	−0.62	−0.73
99	−10.01	−23.89	0.00	0.66	0.81	111	−6.41	−10.39	–	−2.71	−1.12
100	−9.68	−18.77	−0.61	0.35	0.08	112	−8.48	−11.44	−1.32	−0.78	−0.97
101	−8.82	−15.37	−0.67	−0.46	−0.41	113	−7.90	−15.68	–	−1.32	−0.36
102	−8.97	−8.05	–	−0.31	−1.45	114	−9.69	−21.66	−0.34	0.36	0.49
103	−9.21	−19.24	−0.65	−0.09	0.15	115	−9.26	−18.67	−0.34	−0.04	0.07
104	−8.69	−20.62	–	−0.57	0.34	116	−8.21	−11.70	−1.36	−1.03	−0.93
105	−10.25	−22.50	0.00	0.88	0.61	117	−8.51	−13.72	−1.08	−0.75	−0.64
106	−7.37	−10.61	–	−1.81	−1.09	118	−9.21	−18.62	−0.41	−0.09	0.06
107	−9.14	−14.83	−0.75	−0.15	−0.48	119	−9.56	−18.00	−0.38	0.23	−0.03
108	−9.63	−19.87	–	0.31	0.24	120	−6.22	−6.29	–	−2.89	−1.70
109	−7.85	−10.88	−1.32	−1.37	−1.05						

Ligand	Glide score	ΔG_{bind} (kcal/mol)	Expt. pIC_{50}	Pred. pIC_{50}[a] (Gscore)	Pred. pIC_{50}[b] (ΔG_{bind})
(d)					
121	−8.50	−16.07	−0.71	−0.75	−0.30
122	−6.73	−12.90	−1.65	−2.41	−0.76
123	−7.72	−16.23	−1.09	−1.49	−0.28
124	−7.68	−15.94	−0.77	−1.52	−0.32

Table 7 continued

Ligand	Glide score	ΔG_{bind} (kcal/mol)	Expt. pIC_{50}	Pred. pIC_{50}[a] (Gscore)	Pred. pIC_{50}[b] (ΔG_{bind})
125	−7.07	−14.72	−1.22	−2.09	−0.50
126	−8.76	−20.35	−0.18	−0.51	0.30

Ligand	Glide score	ΔG_{bind} (kcal/mol)	Expt. pIC_{50}	Pred. pIC_{50}[a] (G-score)	Pred. pIC_{50}[b] (ΔG_{bind})	Ligand	Glide score	ΔG_{bind} (kcal/mol)	Expt. pIC_{50}	Pred. pIC_{50}[a] (G-score)	Pred. pIC_{50}[b] (ΔG_{bind})
(e)											
127	−7.18	−13.22	−2.00	−1.99	−0.71	141	−11.18	−27.83	2.74	1.76	1.38
128	−7.41	−15.09	−1.90	−1.78	−0.45	142	−10.85	−29.75	2.77	1.45	1.65
129	−7.71	−11.53	−2.00	−1.50	−0.95	143	−8.11	−17.20	−0.69	−1.12	−0.14
130	−7.88	−13.64	−1.59	−1.34	−0.65	144	−9.28	−18.56	0.12	−0.03	0.05
131	−8.29	−19.66	−0.30	−0.95	0.21	145	−8.78	−22.20	0.11	−0.49	0.57
132	−6.87	−13.81	−1.46	−2.29	−0.63	146	−8.02	−18.22	−0.41	−1.21	0.00
133	−6.71	−10.85	−2.00	−2.43	−1.05	147	−10.48	−28.47	2.39	1.10	1.47
134	−7.63	−12.37	−1.80	−1.57	−0.83	148	−8.99	−19.49	0.04	−0.30	0.18
135	−7.54	−15.25	−1.60	−1.66	−0.42	149	−9.28	−28.47	1.32	−0.02	1.47
136	−7.17	−14.15	−2.00	−2.00	−0.58	150	−9.83	−30.30	2.28	0.49	1.73
137	−7.03	−10.93	−2.00	−2.13	−1.04	151	−8.95	−24.99	0.89	−0.34	0.97
138	−7.38	−16.19	−1.78	−1.81	−0.29	152	−10.74	−27.80	2.28	1.34	1.37
139	−6.92	−10.68	−2.00	−2.24	−1.08	153	−9.14	−29.99	1.52	−0.16	1.68
140	−6.99	−12.37	−1.85	−2.17	−0.83	154	−9.62	−25.29	1.55	0.29	1.01

Expt. Experimental values; *Pred*. predicted values; $pIC_{50} = -\log_{10} IC_{50}$; [a] based on Eq. 3 and [b] as per Eq. 4

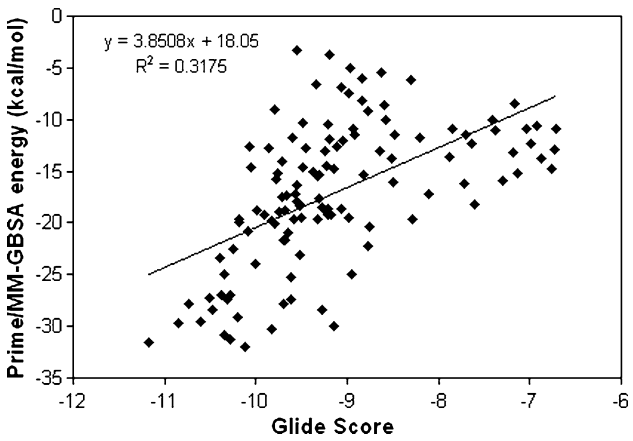

Fig. 4 Relationship between Glide score and Prime/MM-GBSA energy

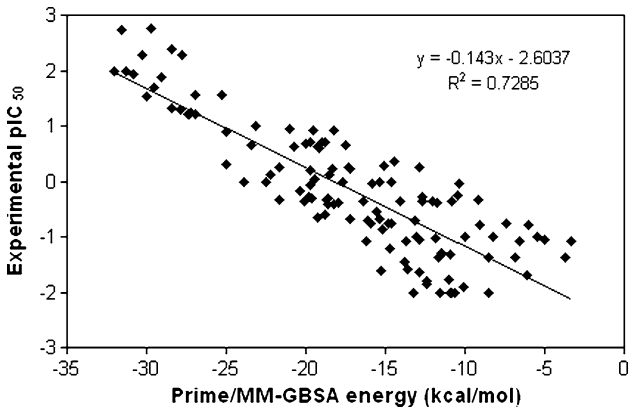

Fig. 5 Models for predicting cytotoxic activity (pIC_{50}) of the podophyllotoxin analogues based on Prime/MM-GBSA energy (ΔG_{bind})

compounds have been seen to be less negative in comparison to lactonic tetralines leading to less potent interaction with tubulin protein and thus lower activity (Table 7). Thus the presence of lactone moiety is very essential for better activity. However, aldehydes at position 9 are more potent than alcohols at this position. This is in accordance with the previous suggestion that an electrophilic group at this position is critical for the possible interaction with the biomolecules. Other transformations on the lactone ring include its reduction leading again to much less cytotoxic compounds and acetylation of the hydroxyl groups does not modify potency [2, 19, 24]. The predicted pIC_{50} values of the analogues calculated based on Glide score and ΔG_{bind} energy value as descriptors are very close to experimental pIC_{50} revealing good prediction models. The pyrazoline and isoxazoline derivatives were less potent than podophyllotoxin as cytotoxicity. Computational techniques based on Glide docking and rescoring using Prime/MM-GBSA also revealed similar conclusion. The pyrazoline derivatives tested so far showed cytotoxicity activity to two and three orders of magnitude lower than those of podophyllotoxin,

Table 8 The experimental IC_{50} value for in vitro tubulin polymerization inhibition by podophyllotoxin analogues

Analogue	Name	Structure	IC_{50} (μM)
1	Podophyllotoxin	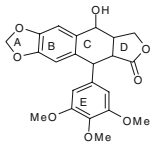	0.6
2	Epipodophyllotoxin	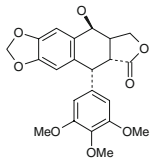	5.0
3	Deoxypodophyllotoxin	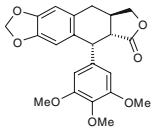	0.5
4	β-Peltatin	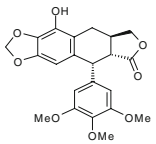	0.7
5	α-Peltatin	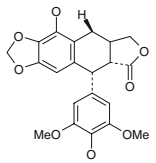	0.5
6	4′-Demethylpodophyllotoxin	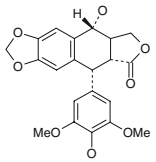	0.5
7	4′-Demethylepipodophyllotoxin	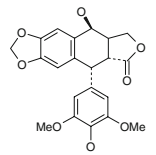	2.0
8	4′-Demethyldeoxypodophyllotoxin	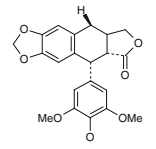	0.2

Table 8 continued

Analogue	Name	Structure	IC_{50} (μM)
9	Dehydropodophyllotoxin	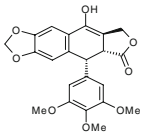	25
10	Anhydropodophyllol	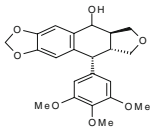	1.0
11	Podophyllotoxin cyclic sulfide	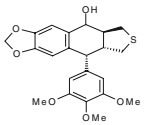	10
12	Podophyllotoxin-cyclic ether	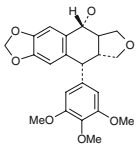	1.0
13	Deoxypodophyllotoxin-cyclic ether	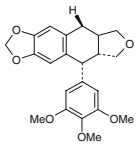	0.8
14	Deoxypodophyllotoxin-cyclopentane	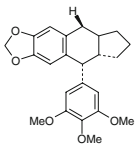	5.0
15	Deoxypodophyllotoxin-cyclopentanone	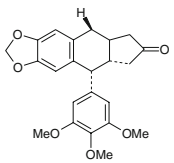	5.0
16	Deoxypodophyllotoxin-cyclic sulfide	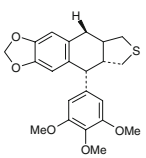	10

The experimental potencies are from literature sources [36, 37]

Table 9 Predicted inhibition of in vitro microtubule assembly by podophyllotoxin analogues using Glide score (XP) and Prime/MM-GBSA energy as a descriptor of podophyllotoxin analogues (16 compounds)

Ligand	Glide score	ΔG_{bind} (kcal/mol)	Ext. pIC_{50}[a]	Pred. pIC_{50}[b]	Pred. pIC_{50}[c]
Podophyllotoxin	−9.54	−19.62	0.22	0.22	0.20
Epipodophyllotoxin	−9.03	−14.37	−0.70	−0.26	−0.55
Deoxypodophyllotoxin	−9.44	−21.15	0.30	0.12	0.42
β-Peltatin	−8.88	−19.34	0.15	−0.40	0.16
α-Peltatin	−9.09	−20.96	0.30	−0.20	0.39
4′-Demethylpodophyllotoxin	−9.70	−19.70	0.30	0.37	0.21
4′-Demethylepipodophyllotoxin	−8.75	−17.46	−0.30	−0.52	−0.11
4′-Demethyldeoxypodophyllotoxin	−9.54	−22.64	0.70	0.21	0.63
Dehydropodophyllotoxin	−7.74	−10.93	−1.40	−1.47	−1.04
Anhydropodophyllol	−9.35	−17.70	0.00	0.04	−0.07
Podophyllotoxin cyclic sulfide	−8.10	−14.24	−1.00	−1.13	−0.57
Podophyllotoxin-cyclic ether	−9.53	−16.63	0.00	0.21	−0.23
Deoxypodophyllotoxin-cyclic ether	−9.35	−22.28	0.10	0.04	0.58
Deoxypodophyllotoxin-cyclopentane	−8.70	−14.26	−0.70	−0.57	−0.56
Deoxypodophyllotoxin-cyclopentanone	−8.62	−16.48	−0.70	−0.64	−0.25
Deoxypodophyllotoxin-cyclic sulfide	−8.27	−13.47	−1.00	−0.97	−0.68

[a] *Expt*. Experimental values; $pIC_{50} = -\log_{10} IC_{50}$

[b] *Pred. pIC_{50}* Predicted pIC_{50} based on Glide score and was calculated using Eq. 3

[c] *Pred. pIC_{50}* Predicted pIC_{50} based on Prime energy and was calculated using Eq. 4

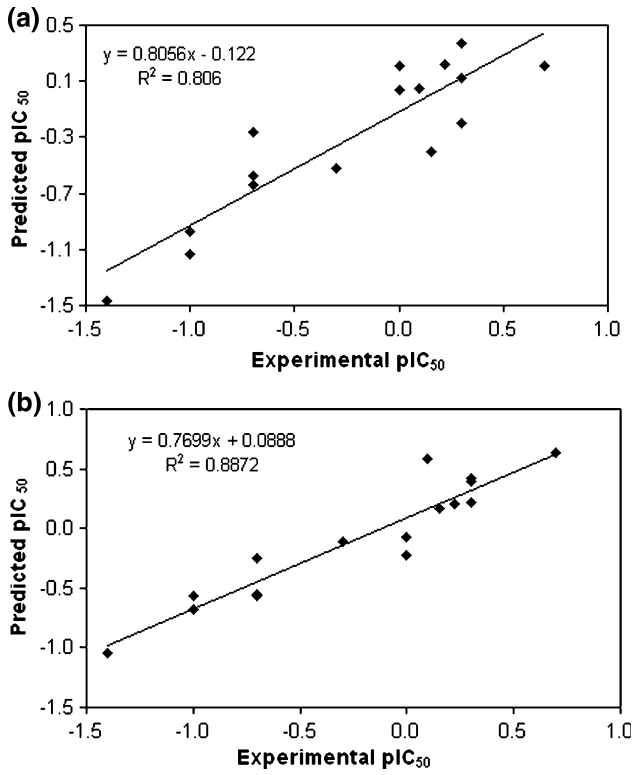

Fig. 6 Relationship between experimental and predicted pIC50 values of the validation set (16 compounds) using (**a**) Glide score and (**b**) Prime/MM-GBSA energy

thus confirming that the presence of the lactone moiety as a prominent requirement for high cytotoxic activity to be achieved. The lactonic and non-lactonic naphthaline group of derivatives has proportionately much lower activity [19, 20, 24] in comparison to other groups. The Glide score and ΔG_{bind} energy value of this group of compounds are not so good and thus seem to interact with the tubulin protein less efficiently. Aza-podophyllotoxin analogues were generally prepared by selective chemical modification of the two aromatic rings (ring B and E) of natural podophyllotoxin [30]. The Glide score among the ligands of these libraries vary in between −11.18 and −6.71 and the overall difference is also very small −5.07. It revealed that these entire ligands bind in tubulin protein with high affinity showed activity (pIC_{50}) in between −2.00 and 2.77 μM. A few aza-podophyllotoxin analogues were proved to be more than twice as cytotoxic as natural podophyllotoxin [30]. Among aza-podophyllotoxin derivatives the best activity, was found for structure 142 ($pIC_{50} = 2.77$ μM) with better Glide score (−10.85) within the library. Similarly, the ΔG_{bind} energy among the ligands of these libraries varies in between −30.30 to −10.68 kcal/mol and the overall difference is also very small (−19.31 kcal/mol). It revealed that all these ligands bind to tubulin protein with high affinity showed activity (pIC_{50}) in between −2.00 and 2.77 μM. Since these groups of analogues bind with tubulin and inhibit microtubule polymerization, the relationship obtained between

Glide score and cytotoxic activity is more probable. Moreover, the linear regression model for prediction of predicted pIC_{50} of cytotoxicity developed by considering Glide score and ΔG_{bind} energy as descriptors (Eqs. 3, 4) seems to be accurate. Reasonably, good agreement between predicted and experimental pIC_{50} is found suggesting that the calculated pIC_{50} based on Glide score and ΔG_{bind} energy are robust and accurate.

Conclusion

We have compiled a virtual library of podophyllotoxin analogues built through structural modification of scaffold structure of natural podophyllotoxin. Docking and rescoring have been done using Prime/MM-GBSA in the work to get insights into ligand:tubulin interactions and corresponding cytotoxic activity of podophyllotoxin analogues. In the docking simulations, the flexible docking reproduced the binding structure of crystal structures well. These experiments verified the docking protocol adopted in the work. Also the docking simulations of structurally similar inhibitors showed that the docking simulation could dock inhibitors into a receptor comparable to the crystal structure complex with podophyllotoxin. Several sets of podophyllotoxin analogues have been studied in the docking simulations. Results showed that these analogues bind in a very similar mode. The magnitude of the binding affinity can be a key factor that decides the activeness of an individual inhibitor. An energetic evaluation of the binding affinity will provide a way to estimate the activity of inhibitors. In any binding energy calculation, the correct binding structure of each ligand has to be determined first prior to binding energy estimation. Only the binding structure of podophyllotoxin with tubulin is available. But the binding structures of the analogues of podophyllotoxin are not available. We use flexible docking to determine the binding structure of the podophyllotoxin analogues with tubulin protein. Very similar binding structures were obtained for a set of analogues. This makes a credible prediction model of the cytotoxic activity (pIC_{50}) calculation possible. The calculated Glide score and binding free energy value of a set of structural analogues demonstrates excellent linear correlation to the experimental cytotoxic activity. These models could be useful to predict the range of activities for new podophyllotoxin analogues. We also found that refinement of poses and consequent rescoring using Prime/MM-GBSA lead to better predictivity of pIC_{50}. The information that we have expressed in this study may lead to the designing (synthesis) of more potent podophyllotoxin derivatives for inhibition of microtubule polymerization.

References

1. Hamel E (1996) Med Res Rev 16:207. doi :10.1002/(SICI)1098-1128(199603)16:2<207::AID-MED4>3.0.CO;2-4
2. Brewer CF, Loike JD, Horwitz SB, Sternlicht H, Gensler WJ (1979) J Med Chem 22:215. doi:10.1021/jm00189a001
3. Jardine I, Cassady JM, Douras JD (1980) In: Cassady JM, Douras JD (eds) Anticancer agents based on natural product models. Academic Press, New York
4. Keller-Juslen C, Kuhn M, von Wartburg A, Stahelin H (1971) J Med Chem 14:936. doi:10.1021/jm00292a012
5. Weiss SG, Tin-Wa M, Perdue RE Jr, Farnsworth NR (1975) J Pharm Sci 64:95. doi:10.1002/jps.2600640119
6. Snyder JA, McIntosh RJ (1976) Annu Rev Biochem 45:699. doi:10.1146/annurev.bi.45.070176.003411
7. Margolis RL, Wilson L (1978) Cell 13:1. doi:10.1016/0092-8674(78)90132-0
8. Cortese F, Bhattacharyya B, Wolff P (1977) J Biol Chem 252:1134
9. David-Pfeuty T, Simon C, Pantaloni D (1979) J Biol Chem 21:2392
10. Lin CM, Hamel E (1981) J Biol Chem 256:9242
11. Whiting DA (1985) Nat Prod Rep 2:191. doi:10.1039/np9850200191
12. PJSr Loehrer (1991) Cancer 67:220. doi :10.1002/1097-0142(19910101)67:1+<220::AID-CNCR2820671303>3.0.CO;2-O
13. Sun L, McPhail AT, Hamel E, Lin CM, Hastie SB, Chang JJ, Lee KH (1993) J Med Chem 36:544. doi:10.1021/jm00057a004
14. Yamashita A, Tawa R, Imakura Y, Shibuya M, Lee KH (1994) Mol Pharmacol 47:1920
15. Schrodinger LLC (2007) http://www.schrodinger.com
16. Polak E, Ribiere G (1969) Revue Francaise Inf Rech Oper, Serie Rouge 16-R1:35
17. San Feliciano A, Miguel del Corral JM, Gordaliza M, Castro MA (1989) Phytochemistry 28:659. doi:10.1016/0031-9422(89)80081-0
18. San Feliciano A, Miguel del Corral JM, Gordaliza M, Castro MA (1990) Phytochemistry 29:1335. doi:10.1016/0031-9422(90)85460-W
19. San Feliciano A, Gordaliza M, Miguel del Corral JM, Castro MA, García-Grávalos MD, Ruiz- Lázaro P (1993) Planta Med 59:246. doi:10.1055/s-2006-959660
20. Gordaliza M, Castro MA, García-Grávalos MD, Ruiz-Lázaro P, Miguel del Corral JM, San Feliciano A (1994) Arch Pharm (Weinheim) 327:175. doi:10.1002/ardp.19943270309
21. Castro MA, Gordaliza M, Miguel del Corral JM, San Feliciano A (1994) Org Prep Proced Int 26:539
22. Gordaliza M, Miguel del Corral JM, Castro MA, López-Vázquez ML, García PA, San Feliciano A, García-Grávalos MD (1995) Bioorg Med Chem Lett 5:2465. doi:10.1016/0960-894X(95)00432-S
23. Miguel del Corral JM, Gordaliza M, Castro MA, Morales LJ, López JL, San Feliciano A (1995) J Nat Prod 58:870. doi:10.1021/np50120a008
24. Doré JC, Viel C, Pageot N, Gordaliza M, Castro MA, Miguel del Corral JM, San Feliciano A (1996) J Pharm Belg 51:9
25. Gordaliza M, Faircloth GT, Castro MA, Miguel del Corral JM, López-Vázquez ML, San Feliciano A (1996) J Med Chem 39:2865. doi:10.1021/jm960023h
26. Gordaliza M, Castro MA, Miguel del Corral JM, San Feliciano A, Faircloth GT (1997) Bioorg Med Chem Lett 7:2781. doi:10.1016/S0960-894X(97)10072-5
27. Gordaliza M, Miguel del Corral JM, Castro MA, López-Vázquez ML, San Feliciano A, García Grávalos MD, Carpy A (1995) Bioorg Med Chem 3:1203. doi:10.1016/0968-0896(95)00091-T

28. Gordaliza M, Castro MA, San Feliciano A, Miguel del Corral JM, López-Vazquez ML, Faircloth GT Patent EP 711765 A1
29. Miguel del Corral JM, Gordaliza M, Castro MA, García-Grávalos MD, Broughton H, San Feliciano A (1997) Tetrahedron 53:6555. doi:10.1016/S0040-4020(97)00310-4
30. Hitotsuyanagi Y, Fukuyo M, Tsuda K, Kobayashi M, Ozeki A, Itokawa H, Takeya K (2000) Bioorg Med Chem Lett 10:315. doi:10.1016/S0960-894X(99)00693-9
31. Friesner RA, Banks JL, Murphy RB, Halgren TA, Klicic JJ, Mainz DT, Repasky MP, Knoll EH, Shaw DE, Shelley M, Perry JK, Francis P, Shenkin PS (2004) J Med Chem 47:1739. doi:10.1021/jm0306430
32. Halgren TA, Murphy RB, Friesner RA, Beard HS, Frye LL, Pollard WT, Banks JL (2004) J Med Chem 47:1750. doi:10.1021/jm030644s
33. Lyne PD, Lamb ML, Saeh JC (2006) J Med Chem 49:4805. doi:10.1021/jm060522a
34. Haar ET, Rosenkranz HS, Hamel E, Day BW (1996) Bioorg Med Chem 10:1659
35. Gordaliza M, Castro MA, Miguel del Corral JM, San Feliciano A (2000) Curr Pharm Des 6:1811. doi:10.2174/1381612003398582
36. ter Haar E, Rosenkranz HS, Hamel E, Day BW (1996) Bioorg Med Chem 4(10):1659. doi:10.1016/0968-0896(96)00158-7
37. Loike JD, Brewer CF, Sternlicht H, Gensler WJ, Horwitz SB (1978) Cancer Res 38:2688
38. San Feliciano A, Miguel del Corral JM, Gordaliza M, Castro MA (1991) Phytochemistry 30:3483. doi:10.1016/0031-9422(91)83240-L